

Rotational and vibrational spectra of quantum rings

M. Koskinen,¹ M. Manninen,¹ B. Mottelson,² and S. M. Reimann¹
¹*Department of Physics, University of Jyväskylä, 40351 Jyväskylä, Finland*
²*NORDITA, Blegdamsvej 17, 2100 Copenhagen, Denmark*

(Received 18 January 2001; published 7 May 2001)

Many-body spectra of quantum rings confining a few electrons are determined by exact diagonalization techniques. Surprisingly, a model of localized electrons accurately describes such systems at rather high electron densities. Group-theoretical methods provide the necessary tools to uncover rotational and vibrational structures in the spectra.

DOI: 10.1103/PhysRevB.63.205323

PACS number(s): 73.21.-b, 73.23.-b, 85.35.Be

One can confine the two-dimensional electron gas in semiconductor heterostructures electrostatically or by etching techniques such that a small electron island is formed. These man-made “artificial atoms” provide the experimental realization of a text-book example of many-particle physics: a finite number of quantum particles in a trap. Much effort was spent on making such “quantum dots” smaller and going from the mesoscopic to the quantum regime.^{1,2} Far-reaching analogies to the physics of atoms, nuclei or metal clusters were obvious from the very beginning. The concepts of shell structure and Hund’s rules were found¹ to apply — just as in real atoms. In this paper, we report the discovery that electrons confined in ring-shaped quantum dots form rather rigid molecules with antiferromagnetic order in the ground state. This can be seen best from an analysis of the rotational and vibrational excitations.

While the independent-particle picture was successful in describing the electronic structure for rather large particle densities, for more dilute systems or in stronger magnetic fields correlation effects are of crucial importance. Configuration-interaction (CI) calculations, which have a long tradition in quantum chemistry and cluster physics, were then much used.³ Although these so-called “exact” calculations are numerically demanding and limited to the smallest sizes, they still are able to provide significant insight into the many-body phenomena that occur in these finite fermion systems with reduced dimensionality. In this paper we apply CI techniques to investigate the electronic structure of *quantum rings* that contain up to seven electrons. Usually the confinement of small, two-dimensional quantum dots is to a very good approximation harmonic. Correspondingly, we model quantum rings as they are realized in the laboratory^{4,5} by a potential of the form $V(r) = \frac{1}{2}m^*\omega_0^2(r-r_0)^2$. For moderate confinement this potential corresponds to an harmonic dot with its center removed. Ground and excited states of N electrons trapped in the potential $V(r)$ are determined from numerical diagonalization as a function of the total angular momentum. Surprisingly, at electron densities and strengths of the ring confinement where one should expect electron *liquid* behavior, a model that assumes *localization* of the electrons in the ring is successful in analyzing the many-body spectra. Group-theoretical methods familiar from molecular physics provide the necessary tools to uncover rotational and vibrational structures in the spectra. The spin sequence and energies of the low-lying states for given an-

gular momentum can be understood from the symmetry associated with the electronic ground-state configuration. It is intriguing that the success of the simple rigid-rotor model for the low-lying states is *not* limited to a regime where the system becomes one-dimensional. The fact that the electrons behave as if they were localized in the ring is reflected in a remarkable agreement of the CI results with the Heisenberg model. Localization at large electron densities has earlier been discussed in parabolic quantum dots, where the interpretation is not yet conclusive.⁶

We write for the Hamiltonian

$$H = \sum_{i=1}^N \left[-\frac{\hbar^2}{2m^*} \nabla_i^2 + V(r_i) \right] + \sum_{i<j}^N \frac{e^2}{4\pi\epsilon_0\epsilon} \frac{1}{|\mathbf{r}_i - \mathbf{r}_j|}, \quad (1)$$

where m^* and ϵ are the effective mass and the dielectric constant of the corresponding semiconductor material. The parameters that determine the properties of the quantum ring are the number of electrons N , the radius of the ring r_0 and the strength ω_0 of the harmonic confinement in the radial direction. The quantities r_0 and ω_0 can be related to the approximate values for the conventional parameters that describe the infinite system: the one-dimensional density parameter r_s describes the particle density $n = 1/(2r_s)$ along the ring (thus $r_0 = Nr_s/\pi$). The parameter C_F is dimensionless and measures the degree of one-dimensionality. C_F essentially describes the excitation energy of the next radial mode $\hbar\omega_0$, which is defined to be C_F times the one-dimensional (1D) Fermi energy. We thus obtain $\hbar\omega_0 = C_F\hbar^2\pi^2/(32m^*r_s^2)$. The higher the value of C_F , the more the radial modes are frozen in their ground states. Thus, the ring is narrower for larger C_F . For the CI calculation, the spatial single-particle states of the Fock space are chosen to be eigenstates of the single-particle part of the Hamiltonian H . We expand them in the harmonic oscillator basis. According to their eigenenergies, from 30 to about 50 lowest single-particle states are selected to span the Fock space. Typically this means that for lower angular momentum states several radial quantum numbers $n=0,1,2,3$ are included, whereas the higher angular momentum states $l = \pm 6, \dots, \pm 10$ have only $n=0$. To set up the Fock states for diagonalization, we sample over the full space with a fixed number of spin-down and spin-up electrons, $N_\downarrow + N_\uparrow = N$. From this sampling, only those states with a given total orbital angular momentum and a configuration energy (corresponding to the sum of occu-

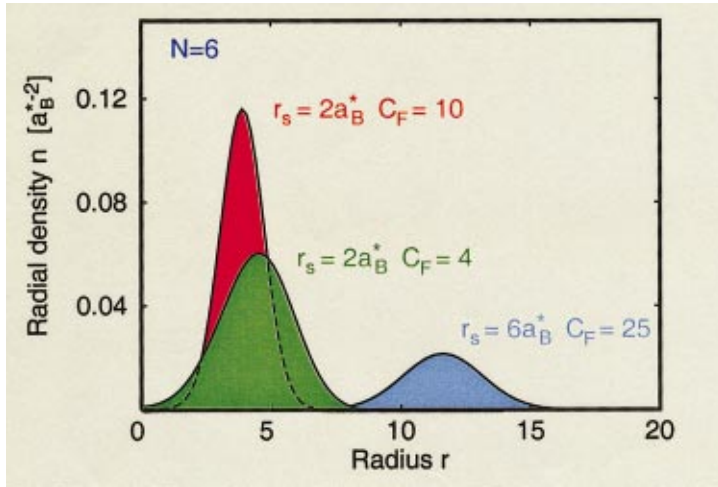


FIG. 1. (Color) Density along the radial direction for $N=6$ and different parameters r_s and C_F . The confinement is moderate for $r_s=2$ and $C_F=4$ (green). The degree of one-dimensionality is enhanced for $C_F=10$ (red). The low-density regime is displayed for $r_s=6$ and $C_F=25$ (blue).

pied single-particle energies) less than the specified cutoff energy e_c are selected. The purpose was to choose only the most important Fock states from the full basis and hereby reducing the matrix dimension to a size $d \leq 2 \times 10^5$. To obtain all the eigenstates with different total spin, we have to set $N_\downarrow = N_\uparrow = N/2$ for even particle numbers ($S_z=0$, all states with different total spin have this component), and analogously $N_\downarrow = N_\uparrow \pm 1$ for odd numbers. Once the active Fock states have been specified, the Hamiltonian matrix is calculated. For diagonalization we use the Arpack library⁹ suitable for large, sparse matrices. Finally, the total spin of each eigenvector is determined by calculating the expectation value of the \hat{S}^2 operator. The many-particle states are characterized by the total orbital angular momentum M and the total spin S . The lowest energy at given angular momentum M defines the so-called “yrast” line, a terminology that was introduced in nuclear physics many years ago.

To begin with, let us look at the energy spectra of a ring with six electrons at a density corresponding to $r_s=2a_B^*$. (Throughout this paper, we use effective atomic units. Taking GaAs as an example, the units of length and energy are $a_B^*=9.8$ nm and a.u. $^*=12$ meV.) For $C_F=4$, the strength of

the ring confinement is moderate, as can be seen from the density distribution displayed in Fig. 1. The system parameters N , r_s , and C_F in this case are chosen such that the rings resemble quite closely structures as they can nowadays be made in the laboratory. For the six-electron ring, Fig. 2 shows the 50 lowest states for all angular momenta from $M=0$ up to $M=6$. The spin configurations are given for the low-lying states. The ground state for $M=0$ has spin $S=0$ and is followed by a state with $S=2$, then $S=1$ and, close in energy, another $S=0$ state. A large energy gap separates these low-lying states from higher bands with a much increased density of states. We note that the sequence of spins of the states below the gap for $M=0$ is *repeated* at $M=6$. (The energy difference between the two $S=0$ states at $M=6$ is slightly reduced, as in a not-very-narrow ring rotation expands the ring.) Inspecting the grouping of the states below the gap for each of the different M values more closely, we see that in a similar way, the states for $M=1$ follow the same sequence as those for $M=5$, and the $M=2$ spectrum is repeated at $M=4$. These sequences of states clearly reveal the spectrum of a dynamical system that can be described, at least approximately, in terms of independent rotation, vibra-

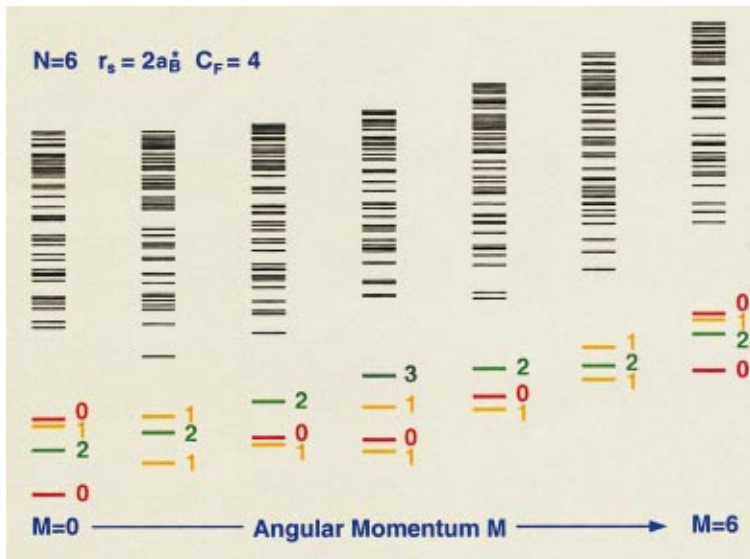


FIG. 2. (Color) Many-body spectra of a quantum ring with $N=6$ electrons ($r_s=2a_B^*$ and $C_F=4$). The energy difference between the yrast states for $M=0$ and $M=6$ is 0.143 a.u. * . The spin S is given for the low-lying states (as also indicated by different colors of the levels).

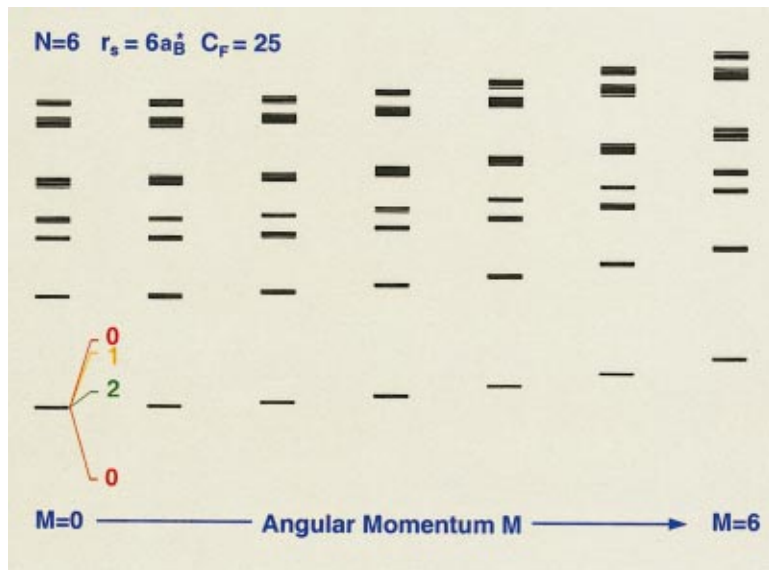


FIG. 3. (Color) Spectra of a narrow low-density quantum ring with six electrons ($r_s=6$ and $C_F=25$), showing the seven lowest vibrational bands. For the vibrational ground state we show the $M=0$ levels in an magnified scale to demonstrate that the energy ratios are the same as in the much wider rings shown in Figs. 2 and 4.

tion and intrinsic spin degrees of freedom. This becomes particularly clear when repeating the above calculation for a much lower particle density in a more narrow ring. We show in Fig. 3 the six-particle spectra for $r_s=6a_B^*$ and $C_F=25$. (The particle density for these parameters is displayed in Fig. 1.) The spectra now indeed consist of narrow bands. The lowest band is the vibrational ground state and consists of the rotational levels. The different spin levels become almost degenerate, as localization has reached a degree where spin-spin interactions become less important. Nevertheless, the sequence of spins and their relative energetic order is similar to the higher density results shown in Fig. 1, as a plot of the low-lying levels at an enlarged energy scale for $M=0$ demonstrates.

We now show that the above spectra can be understood in terms of the standard effective Hamiltonian employed in the interpretation of the rotational and vibrational spectra of planar, polygonal molecules composed of N identical spin 1/2 fermionic atoms.⁷ The standard description is very slightly modified in order to enforce the planarity and the one-dimensionality of the molecule considered here:

$$H_{eff} = \frac{\hbar^2 M^2}{2I} + \sum_a \hbar \omega_a n_a + J \sum_{i,j} \mathbf{S}_i \cdot \mathbf{S}_j, \quad (2)$$

where I is the rigid moment of inertia of the N “atoms” located at the N vertices of an equilateral polygon, ω_a are the vibrational frequencies, and n_a ($=0,1,2,\dots$) the number of excitation quanta of the different normal modes of vibrations; for odd N there are $\frac{1}{2}(N-1)$ twofold degenerate normal modes, while for even N there are $\frac{1}{2}N-1$ twofold degenerate and one nondegenerate modes. The last term in Eq. (2) describes the nearest-neighbor spin-spin interaction that is a result of the exchange term in the interaction of the neighboring fermions (antiferromagnetic Heisenberg model). In the expression (2) we have ignored the contribution of a possible spin-orbit term.

For the $N=6$ molecule discussed in Figs. 2 and 3, the C_{6v} symmetry classification of the normal modes is (in order of

increasing vibrational frequency) E_1 (twofold degenerate), E_2 (twofold degenerate), and B_1 (nondegenerate).⁸ The rotational states carry symmetry for $M \equiv 0$ (A_1 or A_2), $M \equiv 1$ or 5 (E_1), $M \equiv 2$ or 4 (E_2), $M \equiv 3$ (B_1 or B_2), where the congruent sign in all these terms refers to congruent (mod 6),

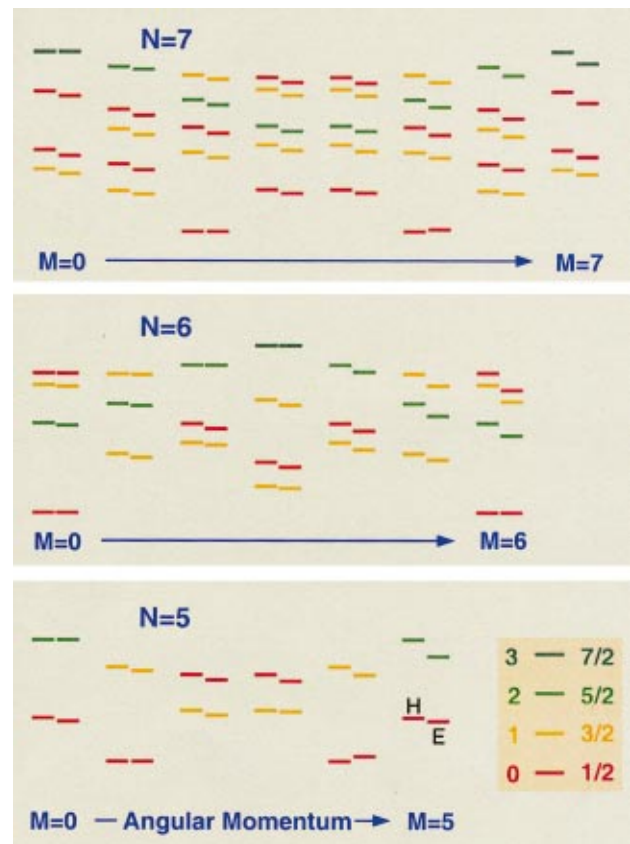


FIG. 4. (Color) Low-lying (rotational) spectra of quantum rings with $N=5, 6,$ and 7 electrons: Comparison between the Heisenberg model (left columns in each of the spectra for given M) and exact diagonalization (right). The spins of the levels are marked by different colors.

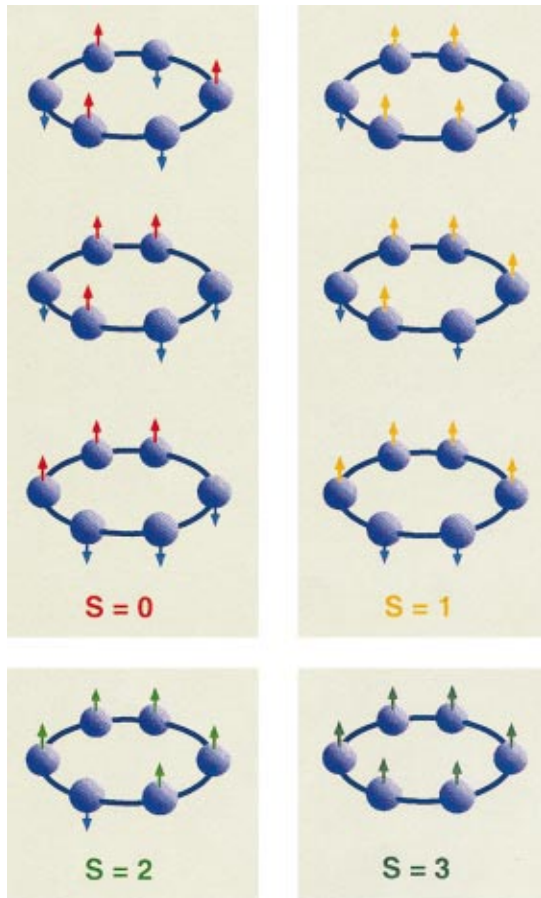


FIG. 5. (Color) Schematic view of the spin configurations in a six-electron ring for different values of S .

and the total wave function must have C_{6v} symmetry B_2 in order to fulfill the requirement of antisymmetry between all the electrons. Thus the spin multiplets occurring for the lowest states at each value of the angular momentum M are determined by the condition that the product of spin and orbital C_{6v} representations must yield the B_2 representation for the total wave function. As we learned from the above analysis, the lowest band is of rotational nature, while the bands above the energy gap represent vibration in addition to rotation. The three vibrational modes of such a system have energy ratios $\omega_1:\omega_2:\omega_3=1:\sqrt{7/3}:\sqrt{3}$, in excellent agreement with the three lowest excitations for $M=0$ shown in Fig. 3. The three highest states have then energies $2\omega_1$, $\omega_1 + \omega_2$, and $\omega_1 + \omega_3$. Figure 4 quantitatively compares the spin dependent part of H_{eff} , Eq. (2), (i.e. The Heisenberg model) to the rotational band of the CI spectra described above. [In the latter case the center-of-mass motion associated to the orbital angular momentum (M^2 -term) is subtracted from

each level. The moment of inertia is determined to make the lowest-energy eigenvalue corresponding to $M=N$ equal to that of $M=0$. The resulting values of I are very close to $I = Nm r_0^2$ obtained for strictly localized electrons. The scale of the Heisenberg result is determined to get the same bandwidth as in the CI case.] Figure 4 displays for electron numbers $N=5,6$, and 7 at $r_s = 2a_B^*$ and $C_F = 10$ the spectra of the states below the first gap that (as analyzed above) all are of rotational nature. For $N=7$, corresponding to the larger particle number, there are now more states as we have more possibilities for the different spin configurations. The above comparison shows that indeed the electrons in a ring can be rather accurately described as localized electrons: *The whole rotational spectrum close to the yrast line can be determined by a spin model combined with a rigid center-of-mass rotation.* It should be noted that the results shown in Fig. 4 are calculated for a ring with a finite width. On making the ring narrower, the remaining small disagreement between the Heisenberg model and exact calculation vanishes.

We finally mention that the pair correlation function does indicate antiferromagnetic coupling of the electrons in the ground state. (See configuration schematically shown in the top left corner of Fig. 5.) However, the correlation is not as clear as expected from the rotational structure in the energy spectrum. In the limit of an infinitely long one-dimensional Heisenberg model the spin-spin correlation decreases as $1/r_{ij}$. Consequently, even in the more narrow rings, where the rotational and vibrational spectra show a clear localization of electrons, the pair correlation function shows only rather weak spin-spin correlation.^{10,11}

In conclusion, we reported rotational and vibrational many-body spectra of quantum rings confining up to seven electrons. We saw that surprisingly, localization occurs in the internal structure of the ground-state many-body wave function. For even electron numbers, antiferromagnetic ordering was found for the ground state. Such so-called spin density waves in quantum rings actually were predicted by density-functional theory.¹² The many-body spectra of the reported exact diagonalization calculations, their analysis by group-theoretical methods and further the comparison to the Heisenberg model confirm that indeed the simple mean-field picture (as it is provided by density-functional theory) can to a rather large degree correctly map out the *internal* symmetry of the many-body wave function.

Note added. We have also recently learned about related work by Borrmann *et al.*¹³ confirming our observation.

This work was supported by the Academy of Finland, the TMR program of the European Community under contract ERBFMBICT972405 and a NORDITA Nordic Project on “Confined Quantum Systems.”

¹S. Tarucha, D.G. Austing, T. Honda, R.J. van der Hage, and L.P. Kouwenhoven, Phys. Rev. Lett. **77**, 3613 (1996).

²L.P. Kouwenhoven *et al.*, in *Proceedings of the Advanced Study Institute on Mesoscopic Electron Transport*, edited by L.L.

Sohn, L.P. Kouwenhoven, and G. Schön (Kluwer, Dordrecht, 1997).

³P.A. Maksym and T. Chakraborty, Phys. Rev. Lett. **65**, 108 (1990); U. Merkt, J. Huser, and M. Wagner, Phys. Rev. B **43**,

- 7320 (1991); P. Hawrylak, *Phys. Rev. Lett.* **71**, 3347 (1993); A.H. MacDonald and M.D. Johnson, *ibid.* **70**, 3107 (1993); S.-R.E. Yang, A.H. MacDonald, and M.D. Johnson, *ibid.* **71**, 3194 (1993); J.J. Palacios *et al.*, *Phys. Rev. B* **50**, 5760 (1994); P.A. Maksym, *ibid.* **53**, 10 871 (1996); T. Ezaki, N. Mori, and C. Hamaguchi, *ibid.* **56**, 6428 (1997).
- ⁴A. Lorke, R.J. Luyken, A.O. Govorov, J.P. Kotthaus, J.M. Garcia, and P.M. Petroff, *Phys. Rev. Lett.* **84**, 2223 (2000).
- ⁵R.J. Warburton, C. Schäfflein, D. Haft, F. Bickel, A. Lorke, K. Karal, J.M. Garcia, W. Schoenfeld, and P.M. Petroff, *Nature (London)* **405**, 926 (2000).
- ⁶R. Egger *et al.*, *Phys. Rev. Lett.* **82**, 3320 (1999); C.E. Creffield *et al.*, *Phys. Rev. B* **59**, 10 719 (1999); C. Yannouleas and U. Landmann, *Phys. Rev. Lett.* **82**, 5325 (1999); S.M. Reimann, M. Koskinen, and M. Manninen, *Phys. Rev. B* **62**, 8108 (2000).
- ⁷G. Herzberg, *Infrared and Raman Spectra of Polyatomic Molecules* (Van Nostrand, New York, 1945).
- ⁸L.D. Landau and E.M. Lifshitz, *Quantum Mechanics: Non-Relativistic Theory* (Pergamon, Oxford, 1977).
- ⁹R.B. Lehoucq, D.C. Sørensen, and Y. Yang, *ARPACK User's Guide: Solution to Large Scale Eigenvalue Problems with Implicitly Restarted Arnoldi Methods*. See <http://www.caam.rice.edu/software/ARPACK>
- ¹⁰D. Vollhardt, in *Perspectives in Many-Particle Physics*, edited by R.A. Broglia, J.R. Schrieffer, and P.F. Bortignon (North-Holland, Amsterdam, 1994).
- ¹¹J.H. Jefferson and W. Häusler, *Phys. Rev. B* **54**, 4936 (1996).
- ¹²M. Koskinen, M. Manninen, and S.M. Reimann, *Phys. Rev. Lett.* **79**, 1389 (1997); S.M. Reimann, M. Koskinen, and M. Manninen, *Phys. Rev. B* **59**, 1613 (1999).
- ¹³P. Borrmann and J. Harting, *Phys. Rev. Lett.* **86**, 3128 (2001).